Molecular Plant • Volume 3 • Number 5 • Pages 904–916 • September 2010 RESEARCH ARTICLE

The Isogene *1-Deoxy-D-Xylulose 5-Phosphate Synthase 2* Controls Isoprenoid Profiles, Precursor Pathway Allocation, and Density of Tomato Trichomes

Heike Paetzold[a], Stefan Garms[b], Stefan Bartram[b], Jenny Wieczorek[a], Eva-Maria Urós-Gracia[c], Manuel Rodríguez-Concepción[c], Wilhelm Boland[b], Dieter Strack[a], Bettina Hause[a] and **Michael H. Walter[a,1]**

a Leibniz Institut für Pflanzenbiochemie, Abteilung Sekundärstoffwechsel, Weinberg 3, D-06120 Halle (Saale), Germany
b Max-Planck-Institut für Chemische Ökologie, Abteilung Bioorganische Chemie, Hans-Knöll-Straβe 8, D-07745 Jena, Germany
c Center for Research in Agricultural Genomics (CRAG), CSIC-IRTA-UAB, Jordi Girona 18, 08034 Barcelona, Spain

ABSTRACT Plant isoprenoids are formed from precursors synthesized by the mevalonate (MVA) pathway in the cytosol or by the methyl-D-erythritol 4-phosphate (MEP) pathway in plastids. Although some exchange of precursors occurs, cytosolic sesquiterpenes are assumed to derive mainly from MVA, while plastidial monoterpenes are produced preferentially from MEP precursors. Additional complexity arises in the first step of the MEP pathway, which is typically catalyzed by two divergent 1-deoxy-D-xylulose 5-phosphate synthase isoforms (DXS1, DXS2). In tomato (*Solanum lycopersicum*), the *SlDXS1* gene is ubiquitously expressed with highest levels during fruit ripening, whereas *SlDXS2* transcripts are abundant in only few tissues, including young leaves, petals, and isolated trichomes. Specific down-regulation of *SlDXS2* expression was performed by RNA interference in transgenic plants to investigate feedback mechanisms. *SlDXS2* down-regulation led to a decrease in the monoterpene β-phellandrene and an increase in two sesquiterpenes in trichomes. Moreover, incorporation of MVA-derived precursors into residual monoterpenes and into sesquiterpenes was elevated as determined by comparison of ^{13}C to ^{12}C natural isotope ratios. A compensatory up-regulation of *SlDXS1* was not observed. Down-regulated lines also exhibited increased trichome density and showed less damage by leaf-feeding *Spodoptera littoralis* caterpillars. The results reveal novel, non-redundant roles of DXS2 in modulating isoprenoid metabolism and a pronounced plasticity in isoprenoid precursor allocation.

Key words: Isoprenoid biosynthesis; methyl-D-erythritol 4-phosphate (MEP) pathway; 1-deoxy-D-xylulose 5-phosphate synthase 2 (DXS2); RNA interference (RNAi); trichomes; cross-talk; feedback regulation; GC–C–IRMS.

INTRODUCTION

In spite of their tremendous diversity in structure and function, all isoprenoids are synthesized from the common C_5 building blocks isopentenyl diphosphate (IPP) and dimethylallyl diphosphate (DMAPP). In plants, these building blocks are produced by two separate routes, located in the cytosol and the plastid compartment, respectively (Lange et al., 2000). The long-known cytosolic mevalonate (MVA) pathway provides precursors for the biosynthesis of sesquiterpenes, polyterpenes, sterols, dolichol, and for ubiquinone formation in mitochondria. The more recently discovered plastidial methyl-D-erythritol 4-phosphate (MEP) pathway supports mainly C_5 supply for the formation of mono- and diterpenes, carotenoids as well as the prenyl moieties of chlorophyll, plastoquinone and tocopherol (Chappell, 2002). The two pathways are thought to be largely independent, but cross-talk has been shown to occur under certain circumstances. For example, the extent of the exchange can be increased by feeding of intermediates of the MVA or the MEP pathways, and by the impairment of one of the pathways with chemical inhibitors,

[1] To whom correspondence should be addressed. E-mail: mhwalter@ipb-halle.de, fax +49-345-5582-1509, tel. +49-345-5582-1520.

doi: 10.1093/mp/ssq032, Advance Access publication 29 June 2010
Received 26 April 2010; accepted 15 May 2010

leading to altered precursor pathway allocations (Jux et al., 2001; Nagata et al., 2002; Hemmerlin et al., 2003; Laule et al., 2003; Schuhr et al., 2003; Bartram et al., 2006). In addition, the synthesis of abundant sesquiterpenes in flowers or trichomes involving strong demand on C_5 supply in the cytosol is supported in part by MEP pathway-derived IPP (Dudareva et al., 2005; Towler and Weathers, 2007; Besser et al., 2009).

The MEP pathway is composed of seven enzymatic reactions starting from pyruvate and glyceraldehyde 3-phosphate (Rodríguez-Concepción and Boronat, 2002; Phillips et al., 2008; Cordoba et al., 2009). The first step is catalyzed by 1-deoxy-D-xylulose 5-phosphate (DXP) synthase (DXS), a transketolase-like enzyme (Lange et al., 1998; Lois et al., 2000). Lack of DXS activity prevents formation of plastidial isoprenoids and strongly impairs plastid biogenesis. The result is an albino phenotype as exemplified by the *Arabidopsis thaliana cla1* mutant, which can be rescued by supplying the dephosphorylated enzyme product (Mandel et al., 1996; Estévez et al., 2000). Overexpression of plant *DXS* genes or introduction of bacterial *DXS* copies can enhance levels of isoprenoid end products (Estévez et al., 2001; Enfissi et al., 2005; Carretero-Paulet et al., 2006; Muñoz-Bertomeu et al., 2006), but can also lead to unexpected perturbations of the isoprenoid metabolic network (Morris et al., 2006). Recently, a *DXS* gene from grapevine (*Vitis vinifera* L.) was found to co-localize with a major quantitative trait locus (QTL) for monoterpene content, important for grape and wine aromas (Battilana et al., 2009; Duchêne et al., 2009). Thus, DXS constitutes a key and bottleneck step in plastidial isoprenoid formation.

The nuclear genes encoding MEP pathway enzymes are generally single copy (Rodríguez-Concepción, 2006; Phillips et al., 2008). The most notable exception is the diversification of *DXS* genes into two structurally distinct, differentially regulated isogenes (Walter et al., 2002). A third, *DXS*-like sequence has been mentioned in this early work, and its expression has further been investigated (Vallabhaneni and Wurtzel, 2009), but its DXS functionality has not been proven. The *DXS1*/*DXS2* diversification is widespread among plant genomes excluding currently only *A. thaliana* (Walter et al., 2002; Kim et al., 2006; Phillips et al., 2008; Kim et al., 2009; Cordoba et al., 2009). The DNA-deduced primary structures of class 1 (DXS1) and class 2 (DXS2) isoforms from various plant species are usually only about 70% identical. The importance of the structural differences is elusive, since both isoforms are functional without any biochemical differences known at this point. However, the striking differences in expression correlated with either normal plant development (primary metabolism, DXS1) or with the formation of isoprenoids important for interactions with the environment (secondary metabolism, DXS2) suggest distinct non-redundant functions in plastidial isoprenoid metabolism (Walter et al., 2002; Kim et al., 2006; Okada et al., 2007; Phillips et al., 2007; Sando et al., 2008; Kim et al., 2009). Such strictly differential and frequently complementary expression patterns of *DXS1* and *DXS2* genes were first described from roots colonized by arbuscular mycorrhizal fungi. Only *DXS2* expression was correlated with the accumulation of certain apocarotenoids during mycorrhization (Walter et al., 2002). In *Medicago truncatula*, the expression of a RNA interference (RNAi) construct targeting *DXS2* in transgenic hairy roots resulted in strong reduction of mycorrhizal apocarotenoid accumulation and was correlated with impairment of symbiotic functions, whereas *DXS1* transcript levels were unaffected (Floss et al., 2008). However, expression of the *DXS2*–RNAi construct was limited to roots in these experiments and a potential impairment of shoot functions by a lack or a depletion of DXS2 activity still needs to be investigated.

Roots of tomato (*Solanum lycopersicum*) colonized by mycorrhizal fungi also exhibit a correlation of *DXS2* expression and apocarotenoid accumulation. However, in contrast to *M. truncatula* and *Zea mays*, elevated levels of *DXS2* transcripts have been found also in tomato leaves (Walter et al., 2002). Tomato leaves contain abundant trichomes, whereas trichome formation is less pronounced in the other two species mentioned. The cloning of a *DXS2*-type gene from trichome-containing peppermint leaves (Lange et al., 1998) and the availability of a multitude of *DXS2*-type ESTs from cDNA libraries from trichome-rich material (see http://compbio.dfci.harvard.edu/tgi/) has led to a tentative assignment of the elevated *DXS2* transcript levels in tomato leaves to trichomes (Walter et al., 2002). Leaves and other organs of tomato develop both non-glandular and glandular trichomes in considerable density. The type VI glandular trichomes with their four-celled heads have been shown to accumulate high levels of monoterpenes and sesquiterpenes and to contribute to insect herbivore resistance (Simmons and Gurr, 2005).

Given the various hints for a potential relevance of *DXS2* expression in tomato trichome isoprenoid formation, we have undertaken a more detailed expression analysis of *DXS* isogenes and their roles in the cultivated tomato variety Moneymaker. To tackle the question of their functional significance, we have carried out a specific knock-down approach on *DXS2* expression in stable tomato transformants. The results obtained extend the scope of *DXS2* expression patterns and the spectrum of potential roles of DXS2. Concerning trichomes, the data demonstrate an unexpected contribution of DXS2 to the control of mono- to sesquiterpene ratios associated with altered utilization of either MEP- or MVA-derived isoprenoid precursors and a role in the regulation of trichome density.

RESULTS

Cloning and Characterization of cDNA and Genomic Sequences of *SlDXS1* and *SlDXS2*

To identify tomato DNA sequences for both DXS isoforms, specific primer pairs were derived from a published *DXS1*–cDNA sequence from *Solanum lycopersicum* (AF143812, Lois et al., 2000) and a putative *DXS2* sequence from a trichome-enriched cDNA library of *Solanum habrochaites* (ShDXS2, AY687353).

Amplification and cloning resulted in two cDNAs referred to as *SlDXS1* and *SlDXS2*. The sequence of *SlDXS1* was fully identical to the published sequence (Lois et al., 2000). Sequence comparison of *ShDXS2* from the database and the amplified *SlDXS2* (FN424052) revealed 98 and 99% identity on the nucleotide and the amino acid level, respectively. Alignment of *SlDXS1* and *SlDXS2* sequences indicates 66 and 69% identity on the nucleotide and amino acid level, respectively. Establishing an amino acid sequence similarity tree of SlDXS isoforms with other plant DXS sequences resulted in the predicted clustering to either class 1- or class 2-DXS sequences (Supplemental Figures 1 and 2; Walter et al., 2002).

To confirm that both the *SlDXS1* and the *SlDXS2* cDNAs encode functional DXS enzymes, a *dxs*-deficient *E. coli* strain (Sauret-Güeto et al., 2006) was used for a complementation analysis. This strain contains a synthetic operon assembled from yeast and human genes that allows bypassing the lethal disruption of the *dxs* gene when mevalonate is added to the growth medium. After transformation with a functional *DXS* sequence, the strain is able to survive without mevalonate. Transformations using cDNA sequences encoding the mature SlDXS1 and SlDXS2 proteins restored the growth of the *dxs*-deficient *E. coli* strains on plates without mevalonate, thereby demonstrating the functionality of both recombinant tomato DXS proteins (Supplemental Figure 3).

To analyze the exon–intron structure of both isogenes, genomic fragments were amplified. In addition, 5′-flanking regions were isolated by a genome walker approach. A total of approximately 4.7 kb (*SlDXS1*, FN424051) and 5.7 kb (*SlDXS2*, FN424052) of genomic sequences was thus obtained. The exon–intron structure is conserved in both isogenes (Supplemental Figure 4). They contain 10 exons and nine introns at positions conserved in other plant species, but the intron sizes vary slightly (Supplemental Figure 4). The available leader and promoter sequences of *SlDXS1* and *SlDXS2* do not exhibit any recognizable extended sequence similarity.

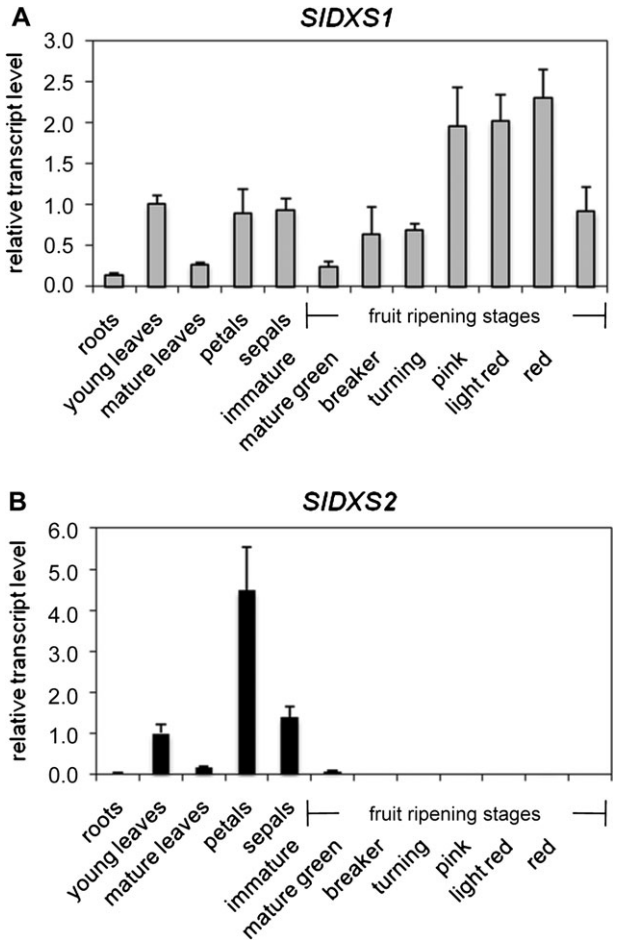

Figure 1. Comparative Analysis of *SlDXS1* and *SlDXS2* Transcript Levels as Determined by Real-time RT–PCR Analyses from Different Tomato Organs.

Each sample is represented by six data points originating from triplicate determinations each of two independent experiments. Error bars indicate SEM. The transcript level of young leaves was set to one for both genes separately.

Organ-Specific Abundance of *SlDXS* Isogene Transcripts and SlDXS Isoform Proteins

A comparative analysis by real-time RT–PCR of *SlDXS1* and *SlDXS2* transcript levels was performed on fully developed tomato plants. *SlDXS1* transcripts were detectable in all organs and tissues tested, including roots, leaves, flower organs, and fruits (Figure 1). Young leaves showed increased *SlDXS1* transcript levels compared to mature leaves, but the highest levels of *SlDXS1* transcripts were found in later stages of fruit ripening correlating with the known massive production of carotenoids (Lois et al., 2000). A very different pattern was obtained for *SlDXS2* transcripts. These were hardly or not detectable in roots, mature leaves, and all stages of fruit ripening, whereas high levels were found in petals (Figure 1). Tomato petals are known to accumulate yellow xanthophylls (Galpaz et al., 2006). Abundant *SlDXS2* transcripts were also found in trichome-rich organs such as young leaves and sepals (Figure 1). To analyze *SlDXS2* transcript-containing organs in more detail, these organs were dissected. Trichomes were isolated from leaves and subjected to RNA isolation followed by real-time RT–PCR. The trichome fraction of leaves clearly exhibited much higher levels of *SlDXS2* than *SlDXS1* transcripts (Figure 2). Unexpectedly, whole stamens of open mature flowers contained high levels of *SlDXS2* transcripts (Figure 2). Stamen and pistils isolated from immature closed flowers showed only low transcript levels of both *SlDXS* genes (data not shown). Pollen isolated from mature stamens did not show a noticeable increase in transcripts of either *SlDXS* isogene. However, when pollen were incubated in germination media prior to RNA extraction, elevated *SlDXS2* transcript levels could be documented, while *SlDXS1* transcripts remained below detection levels (Figure 2).

To monitor the abundance of SlDXS2 isoforms at the protein level, a peptide antibody specific for SlDXS2 was generated. The antibody was used in Western blot analyses against tomato protein extracts from various organs and tissues. The

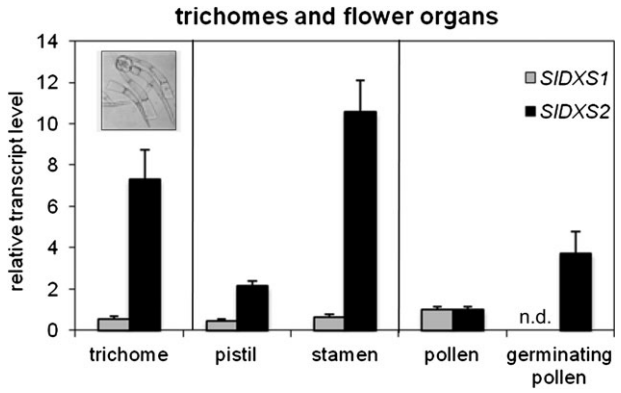

Figure 2. Relative Transcript Levels of *SlDXS1* and *SlDXS2* in Isolated Trichomes and in Flower Organs.

Left panel: RNA from trichomes isolated from leaves. A microscopic image of the trichome fraction after separation from whole leaves is inserted. Center and right panels: RNA samples isolated from open flower parts using whole pistils and whole stamens forming a yellow cylinder around the carpels. Mature pollen collected from stamens; pollen germinated *in vitro*. Determinations and statistics were as described in Figure 1. Reference samples (set to one) were young leaves except for pollen, in which non-germinating pollen was set to one; n. d., not detectable.

highest abundance of SlDXS2 was found in young leaves, but isolated trichomes also showed a protein band at approximately 70 kDa, the calculated size of mature SlDXS2 protein (Figure 3A). The faintness of the signal from the latter sample is probably due to losses during trichome preparation and to many non-glandular trichomes present in the preparation. Samples from red fruit lacked the SlDXS2 protein band (Figure 3A). The overall organ-specific alterations in SlDXS2 at the protein level did thus not considerably deviate from the transcript analyses. The antibody was also tested against purified recombinant SlDXS1 and SlDXS2 proteins, confirming its specificity for SlDXS2 (Figure 3B). It was further used in immunolocalization experiments on leaf material. Immunostaining of semi-thin sections of young leaves revealed an occurrence of SlDXS2 protein in the head cells of glandular trichomes (Figure 3C and 3D).

Specific Knock-Down of *SlDXS2* Expression by RNAi in Transgenic Tomato Plants

To further investigate the role of DXS2, stable transformants expressing a *SlDXS2*-specific RNAi construct were generated. A 262-bp fragment covering the 3′-untranslated sequence and few nucleotides of the C-terminal coding region was introduced into tomato via *Agrobacterium tumefaciens*-mediated transformation. Two transgenic *SlDXS2*–RNAi lines exhibiting significant reduction of *SlDXS2* transcripts in leaves were selected for further investigations. The *SlDXS2*–RNAi line 10 exhibited residual *SlDXS2* transcripts of 8%, whereas *SlDXS2*–RNAi line 13 was reduced to 19% of empty vector controls (Figure 4). In both cases, *SlDXS1* transcript levels were not affected. There were no obvious major alterations in growth

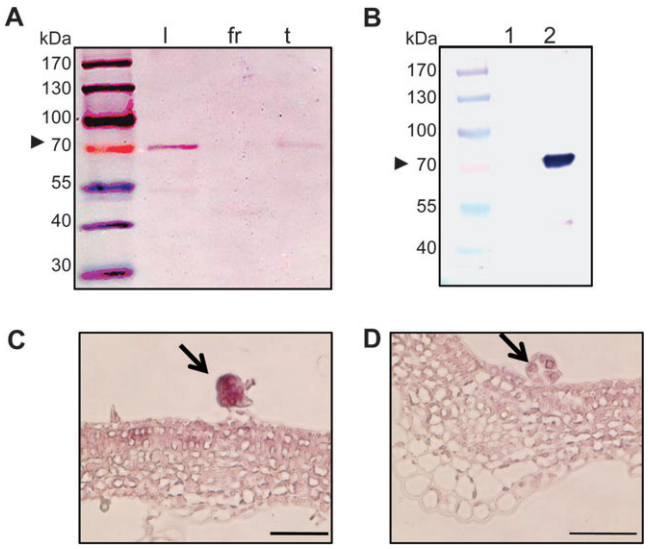

Figure 3. Analysis of SlDXS2 Proteins on Immunoblots and by Immunolocalization.

(A) Protein extracts from whole leaves (l), red fruit (fr), and isolated trichomes (t) separated by SDS–PAGE, immobilized on a PVDF membrane, and treated with the SlDXS2 antiserum.

(B) Purified recombinant SlDXS1 (1) and SlDXS2 protein (2) analyzed with the SlDXS2 antiserum. 200 ng of each protein were loaded onto the gel. The calculated molecular weight of the mature SlDXS2 isoform (approximately 70 kDa) is marked by arrowheads.

(C, D) Immunolocalization of SlDXS2 protein in tomato leaf sections using the SlDXS2 antiserum as primary antibody followed by treatment with a secondary antibody coupled to alkaline phosphatase. (C) Immunostaining using SlDXS2 antiserum; (D) control immunostaining using SlDXS2 antiserum saturated with the antigen peptide prior to treatment. Trichome head cells are marked by arrows. Note the immunodecorated SlDXS2 visualized by dark-purple staining in head cells of a type VI trichome in (C). Bars represent 50 μm.

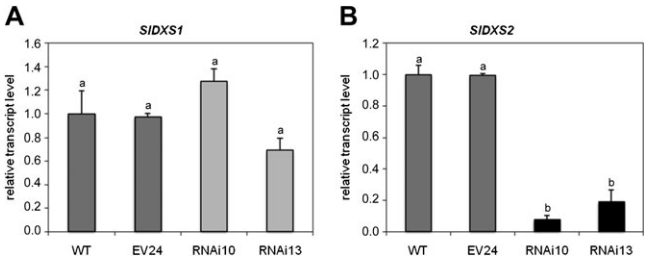

Figure 4. Transcript Levels of *SlDXS1* and *SlDXS2* in Transgenic Lines Suppressed for *SlDXS2* Expression.

The two RNAi lines (RNAi10, RNAi13) are compared with the wild-type (WT, set to one as reference point) and a transgenic control transformed with the empty vector (EV24). The RNA for the real time RT–PCR measurements was obtained from young leaves. Columns represent mean ± SEM ($n = 3$). Values with different letters differ significantly from each other ($P < 0.01$).

and flowering of T_0 transgenic *SlDXS2*–RNAi plants compared to empty vector controls and untransformed plants.

Responsiveness of *DXS2* gene expression to wounding and methyl jasmonate has recently been reported from several

systems (Sánchez-Hernández et al., 2006; Arimura et al., 2008; Tretner et al., 2008; Kim et al., 2009). Therefore, a mechanical wounding experiment was performed on leaves of wild-type and empty vector plants in comparison to the two *SlDXS2* RNAi lines. *SlDXS2* transcript levels of wild-type and empty vector plants were elevated by the wounding treatment. A wound-induced increase in *SlDXS2* transcripts was also observed in the RNAi lines, yet it occurred from a lower base level to a lower induced level than the empty vector and wild-type controls (Figure 5A). This indicates that the wound-responsiveness of *SlDXS2* in RNAi plants is still present but occurs at significantly reduced overall transcript abundance. *SlDXS1* transcript levels were not affected by wounding in the various samples (data not shown). To confirm a successful wounding treatment, transcript levels of an independent wound-inducible gene were determined from all samples. This reference gene was *Allene Oxide Cyclase* (*AOC*; Ziegler et al., 2000) involved in jasmonate biosynthesis. *SlAOC* showed a strong increase in transcript abundance upon wounding, which was not altered in the two RNAi lines (Figure 5B).

SlDXS2 Knock-Down Alters Monoterpene Accumulation and Ratios of MEP to MVA Pathway Allocation

Because SlDXS2 accumulates in trichomes (Figure 3), we next tested whether a reduced accumulation of *SlDXS2* transcripts in RNAi lines may have caused alterations in trichome function. We first investigated whether isoprenoid volatile formation was affected in transgenic plants using a solid phase microextraction-like (SPME-like)-GC–Combustion–MS analysis. Trichome content of leaves was collected on a polydimethylsiloxane (PDMS) tubing and subjected to GC–C–MS analysis. One monoterpene (β-phellandrene) and two sesquiterpenes ((*E*)-β-caryophyllene, α-humulene), known as major isoprenoid compounds of tomato trichomes, were determined from empty vector control plants and the two RNAi lines. β-Phellandrene content was significantly lower in the two RNAi lines (approximately two-fold) compared with the empty vector control, whereas the content of the sesquiterpene (*E*)-β-caryophyllene exhibited a clear trend in the opposite direction (Figure 6A). The abundance of the second sesquiterpene α-humulene was much lower but also showed a similar upwards trend. Overall, in a background of slightly reduced total amounts of the three isoprenoids combined, the ratio

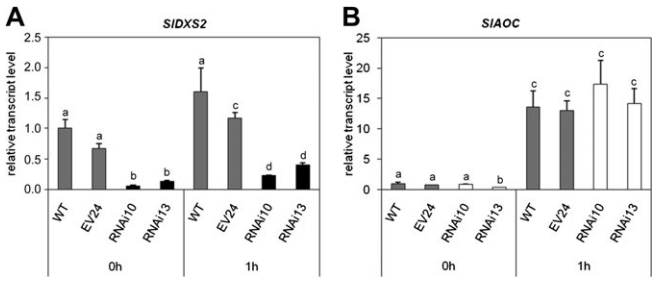

Figure 5. Wound-Induced Transcript Accumulation in Wild-Type (WT), Empty Vector Transgenic (EV24), and *SlDXS2*-Suppressed RNAi Lines (RNAi10, RNAi13).

Samples were taken prior to treatment (0 h) and 1 h after wounding.
(A) *SlDXS2* transcript level determined by real-time RT–PCR.
(B) Transcript levels of *Allene Oxid Cyclase (AOC),* a wound-induced gene used as a control for wound treatment.
Columns represent means ± SEM (n = 3); values with different letters differ significantly from each other ($P < 0.01$). Wild-type samples are again reference point.

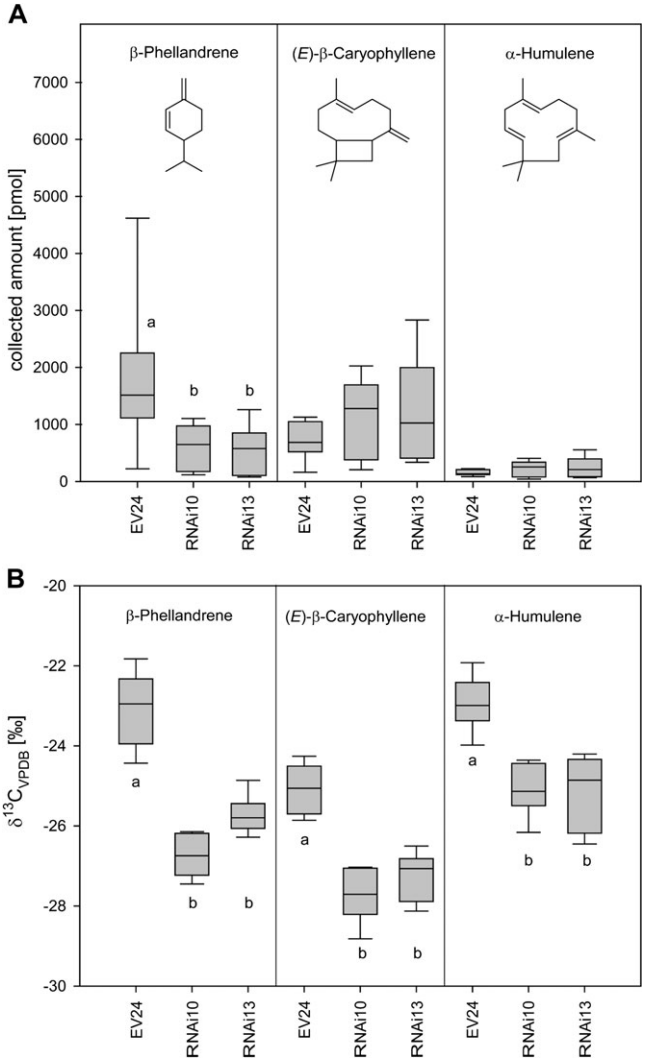

Figure 6. Box-Whisker Plots Comparing Isoprenoid Product Analysis from Empty Vector Control Plants (EV24) and the *SlDXS2*–RNAi10 and RNAi13 Transgenic Lines.

One monoterpene (β-phellandrene) and two sesquiterpenes ((E)-β-caryophyllene and α-humulene) were characterized by two analytical methods.
(A) Total content per leaf of the isoprenoids indicated in trichomes of untreated leaves collected by touching trichomes with a PDMS fiber followed by GC–C–MS analysis. Quantification was performed via a calibration procedure using decane as external standard.
(B) ^{13}C to ^{12}C isotope ratio analysis of isoprenoid products (δ-notation, ‰ scale, see text for details); n = 9 for both (A) and (B). Values with different letters differ significantly from each other ($P < 0.01$).

of sesquiterpenes to monoterpenes was significantly elevated in the RNAi lines.

To investigate whether this increase in sesquiterpene accumulation was accompanied by an altered utilization of MVA-derived precursors, an isotope ratio mass spectroscopy (IRMS) analysis comparing the natural abundance ratio of ^{13}C to ^{12}C in the various samples was performed. The isotope ratio (δ-notation, deviation from the international standard VPDB in ‰) usually varies around –26‰ to –30‰ for monoterpenes and is as low as –37‰ for certain sesquiterpenes (Jux et al., 2001). A depletion in ^{13}C resulting in a more negative $\delta^{13}C$ value is indicative of MVA origin of the IPP of sesquiterpenes, whereas a higher value of $\delta^{13}C$ would indicate increased origin from the MEP pathway. Comparison of $\delta^{13}C$ values between empty vector controls and the two RNAi lines clearly showed a depletion in ^{13}C for all compounds (Figure 6B), consistent with an elevated incorporation of MVA-derived IPP into both the residual monoterpene and the two sesquiterpenes in transgenic plants. Surprisingly, α-humulene exhibited a $\delta^{13}C$ value similar to β-phellandrene in the empty vector control plants (Figure 6B).

Reduced *SlDXS2* Expression Impacts Herbivore Feeding Behavior and Trichome Density

When the various tomato lines were used to feed larvae of the lepidopteran caterpillar *Spodoptera littoralis*, determination of the three abundant isoprenoid compounds by head space analysis indicated a similar trend to that in the PDMS fiber analysis of leaves, namely the emission of fewer monoterpenes and a relative increase in sesquiterpenes in the RNAi lines, but due to large variations, the alterations were not significant (Supplemental Figure 5). Unexpectedly, the leaf area consumed by *S. littoralis* was significantly lower in the two RNAi lines compared to empty vector controls (Figure 7). Given the specific accumulation of DXS2 protein in glandular trichome heads (Figure 3C), potential alterations in trichome characteristics were monitored. There was no obvious *SlDXS2*-suppression-dependent change in morphology of the type VI trichomes, which are characterized by their short stalks and their four-celled heads. However, the number of these glandular trichomes appeared to be elevated in the RNAi lines. Counting of type VI glandular trichomes indicated a significant increase in both RNAi lines compared to wild-type and empty vector control plants (Figure 8A). An environmental scanning electron microscopic (ESEM) analysis of leaves from either wild-type (Figure 8B) or the RNAi10 line (Figure 8C) visualizes the increase in trichome density.

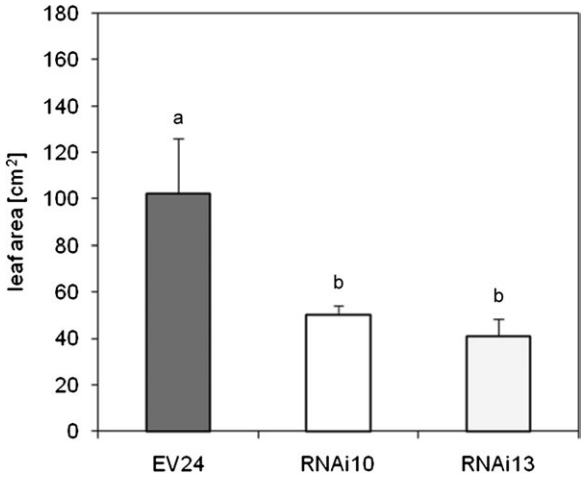

Figure 7. Leaf Area Consumed by Herbivorous *S. littoralis* Caterpillars on Empty Vector Control and SlDXS2 RNAi Plants. Columns represent mean ±SEM of leaf area fed by caterpillar within 48 h. Different letters indicate significant differences ($P < 0.05$; $n \geq 4$).

DISCUSSION

The requirement for DXS activity in plant development and during responses to environmental challenges is met by at least two separate DXS isoforms. These are encoded by differentially regulated genes in the vast majority of angiosperms and gymnosperms (Kim et al., 2006; Sánchez-Hernández et al., 2006; Okada et al., 2007; Phillips et al., 2007; Arimura et al., 2008; Sando et al., 2008; Tretner et al., 2008; Kim et al., 2009). As shown in Supplemental Figure 1, plant DXS amino acid sequences from some of the older reports can now be assigned to class 2 (Lange et al., 1998; Moehs et al., 2001; Totte et al., 2003). Moreover, some new reports not specifying the DXS class in fact also deal with class 2 DXS (Dudareva et al., 2005; Kishimoto and Ohmiya, 2006; Besser et al., 2009). Including two *Arabidopsis* DXS-like (DXSL) sequences in the tree (At3g21500 and At5g11380, previously termed DXSL2 and DXSL3 (Phillips et al., 2008)) shows them to both cluster outside the DXS2 clade (Supplemental Figure 1). This renders *Arabidopsis* the only genome, thus far confirmed for the absence of a *DXS2* gene copy. The results, reported here on the expression of the tomato genes encoding class 1 (SlDXS1) and class 2 (SlDXS2) isoforms (Figures 1, 2, and 3), largely confirm the current model that DXS1 isoforms are preferentially involved in the production of plastidial isoprenoids for housekeeping functions, whereas DXS2 isoforms participate in the production of secondary metabolites, which modulate the interaction of plants with their environment (Walter et al., 2002). Novel examples of elevated *DXS2* expression in plant organs are petals, stamens, pistils, and germinating pollen (Figures 1 and 2). Whether the isoprenoid products, produced from these DXS2 activities, also serve ecological functions remains to be determined. The observations of cell-specific *DXS2* promoter activity in arbusculated cells (Floss et al., 2008) and DXS2 protein accumulation specifically in head cells of glandular trichomes (Figure 3C) also suggest a possible role for DXS2 in meeting strong demand of single cells for isoprenoid precursors.

One exception to the rule of DXS2 assignment to secondary metabolism appears to be the distribution of DXS isoforms during carotenoid biosynthesis in fruits. All stages of tomato

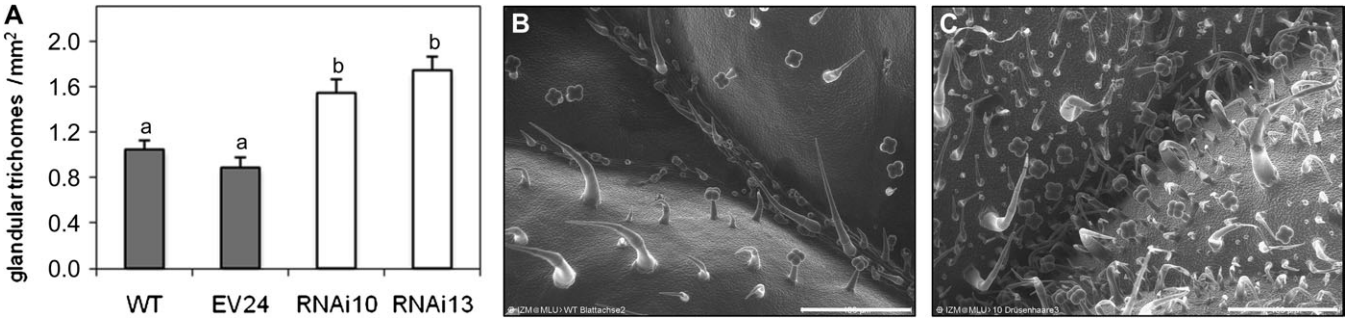

Figure 8. Comparison of Glandular Trichome Numbers in Wild-Type (WT), Empty Vector (EV24), and the SlDXS2-Suppressed RNAi Lines.
(A) Glandular trichomes (type VI) counted from leaves with equal developmental status. Columns represent mean ±SEM; values with different letters differ significantly from each other ($P < 0.05$), $n \geq 10$.
(B–C) Environmental scanning electron micrographs of the leaf surface of a wild-type leaf (B) and a leaf from the transgenic line RNAi10 (C). Type VI trichomes can be identified by their four-celled head sitting on a short stalk. For both plants, similar regions of leaves from the same developmental stage are shown. Bars represent 400 μm.

fruit ripening and in particular the phase of strong lycopene accumulation are correlated with high transcript levels of *SlDXS1* but not *SlDXS2* (Figure 1). Strong accumulation of *SlDXS1* transcripts during tomato fruit ripening has been shown earlier (Lois et al., 2000) but information on *SlDXS2* expression was not previously available. At first sight, a discrepancy is coming up in the use of DXS forms in fruit ripening between tomato and the monocot oil palm *Elaeis guineensis*, which also accumulates carotenoids in the fruit. Transcript levels of a gene termed '*DXS2*' were high in the ripening palm fruit but transcripts of a '*DXS1*' gene were not (Khemvong and Suvachittanont, 2005). However, placing the oil palm '*DXS2*'-deduced amino acid sequence into a DXS sequence similarity tree shows it to be a DXS1 variant and to cluster away from the conserved DXS2 branch described (unpublished results; Walter et al., 2002; see Supplemental Figure 1). Therefore, the oil palm '*DXS2*' appears to represent a specific second *DXS1*-type isogene highly expressed during fruit ripening and should rather be called *DXS1-2* or *DXS1B*. Moreover, the QTL of grapevine determining monoterpene content in grape berries and wine harbors a *DXS1*-type gene (Battilana et al., 2009; Duchêne et al., 2009).

In the main focus of this work, we have experimentally confirmed previous predictions on the participation of a DXS2 isoform in the production of isoprenoids in trichomes (Lange et al., 1998; Walter et al., 2002; Besser et al., 2009). Besides showing an enrichment of SlDXS2 transcript and protein levels in isolated trichomes (Figures 2 and 3A), we observed a clear immunostaining in glandular heads of type VI trichomes using an antibody that recognizes the SlDXS2 isoform (Figure 3C). To investigate the consequences of *SlDXS2* knock-down for trichome isoprenoid constituents, GC–MS analyses were performed after collecting volatiles and semi-volatiles on a PDMS fiber using three-fold repetitions and many biological replicates. Sampling of trichome gland contents by such SPME fiber techniques is a method previously applied to various Lamiaceae (Grassi et al., 2004; Schmiderer et al., 2008). The finding of significantly reduced total and relative content of the monoterpene β-phellandrene in comparison to sesquiterpenes in RNAi lines is consistent with the known role of DXS2 and the MEP pathway in monoterpene biosynthesis (Figure 6A; Lange et al., 1998). Conversely, two sesquiterpenes took over an increased share of total isoprenoids in trichomes of *SlDXS2*-suppressed untreated leaves (Figure 6A). A similar trend for a shift from mono- to sesquiterpene synthesis was observed from an independent sampling method by collecting headspace volatiles during herbivore feeding (Supplemental Figure 5).

In the same context of potential isoprenoid precursor exchange and compensation mechanisms between the MVA and the MEP pathways, the results from determining ^{13}C to ^{12}C natural isotope ratios argue for an increased incorporation of MVA-derived precursors in the RNAi plants (Figure 6B). This elevated contribution of the MVA pathway during the knock-down of the DXS2-dependent part of the MEP pathway applies to both mono- and sesquiterpenes. However, there was a surprising discrepancy between the two sesquiterpenes in that α-humulene had similar natural isotope ratios in both EV24 and RNAi plants as the monoterpene β-phellandrene (Figure 6B). One possible explanation could be substantial MEP pathway contribution to its synthesis in empty vector-transformed and wild-type plants. Even (*E*)-β-caryophyllene with a stronger bias to MVA incorporation in EV24 plants exhibited a shift towards more MVA-derived building blocks in the RNAi plants suppressed for MEP pathway activity. This may indicate that both sesquiterpenes already normally contain MEP-derived precursors, yet to a different extent. In cell cultures of *Catharanthus roseus*, phytosterols, typically attributed to MVA pathway-mediated synthesis, contain as little as 6% MEP-derived precursors (Arigoni et al., 1997). Various ratios of MEP-derived C_5 units are found in sesquiterpenes of *A. majus*, *Artemisia annua*, and *S. habrochaites* (Dudareva et al., 2005; Towler and Wheathers, 2007; Besser et al., 2009).

A recent report from *S. habrochaites* suggests that plastidial MEP-derived IPP may be incorporated into sesquiterpenes not only after its unidirectional transport from the plastid to the cytosol, but also inside the plastid via the concerted action of

plastidial prenyltransferases and sesquiterpene synthases using *cisoid* substrates (Sallaud et al., 2009). *Cisoid* substrates are also novel intermediates recognized in monoterpene biosynthesis in *S. lycopersicum* glandular trichomes (Schilmiller et al., 2009). Different monoterpenes and sesquiterpenes thus appear to be synthesized via different routes, from different substrates and in different compartments. Upon knock-down of MEP-derived IPP supply, as imposed here, the ratios of the various mono- and sesquiterpenes seem to be adjusted depending on the origin of their building blocks. As shown in Figure 6B, the residual amount of β-phellandrene produced is not exclusively provided by residual activity of the MEP pathway, but receives an increased share of MVA-derived IPP. Taken together, the results of the present study, obtained from a non-invasive reverse genetic approach, independent of chemical pathway suppression or feeding labeled intermediates, cannot be explained by a simple two-compartment model of isoprenoid precursor pathways. They rather support a concept of flexible use of resources and a pronounced dynamics of resource allocation within a complex regulatory network, as has been suggested earlier from inhibitor studies in the lima bean system (Bartram et al., 2006).

The question thus arises of whether there might be a compensatory up-regulation of the MVA pathway in *SlDXS2* RNAi plants. The MVA enzyme 3-hydroxy-3-methylglutaryl-coenzyme A reductase (HMGR) catalyzes the main regulatory step of the pathway (Narita and Gruissem, 1989; Stermer et al., 1994). We have performed preliminary analyses of transcript levels of three tomato *HMGR* isogenes (TC 205118 (*SlHMGR1*); TC192597 (*SlHMGR2*) TC196149 (*SlHMGR3*)) tentatively identified from the DFCI database (http://compbio.dfci.harvard.edu/) but high variability has prevented concluding on their potential alterations in RNAi plants. Considering a recent report on posttranslational regulation of HMGR in response to inhibition of sphingolipid and sterol pathways (Nieto et al., 2009), a potential up-regulation of the MVA pathway in SlDXS2-depleted tomato plants should be addressed by analysis of both transcriptional and posttranscriptional levels, which goes beyond the scope of the current work. While it is still unclear whether and how the MVA pathway is induced to rescue isoprenoid biosynthesis in DXS2-depleted tomato trichomes, no up-regulation of *SlDXS1* expression was observed in any of the various experiments to compensate for the reduced transcript levels of *SlDXS2* in the RNAi lines.

Another striking consequence of reducing SlDXS2 levels was a significant increase in the average number of glandular trichomes per mm^2 of leaf area in the tomato RNAi lines (Figure 8A). The trend towards more total sesquiterpenes (Figure 6A) could thus be explained by the higher trichome numbers as an alternative to up-regulation of the MVA pathway, while total and individual trichome production of the monoterpene β-phellandrene is significantly compromised. The volatile headspace analysis largely confirmed the alterations observed via PDMS sampling, although large variations prevent a final statistical proof (Supplemental Figure 5). The increased trichome density might be the decisive parameter to explain the unexpected increased resistance of the transgenic plants to *S. littoralis* feeding (Figure 7). The *hairless* mutation in tomato trichome density and morphology results in reduced densities of type I and type VI trichomes correlated with decreased resistance to a specialist herbivore (Kang et al., 2010). However, the sesquiterpene content of mutant glands was also reduced, impeding a conclusion on the resistance mechanism. Nevertheless, trichome density has been identified as a factor determining herbivore resistance in other cases (Boughton et al., 2005; Maluf et al., 2007). Highly herbivore-resistant wild tomato species often have higher trichome densities in addition to the presence of more defense compounds relative to cultivated species (Simmons and Gurr, 2005). Trichome density is not only dependent on the developmental stage of the leaf, but has also been shown to be affected by other stimuli such as jasmonates. Boughton et al. (2005) have shown that treatment of tomato leaves with jasmonic acid methyl ester can strongly enhance trichome densities, especially that of the type VI trichomes. Moreover, trichome density might also be regulated by the isoprenoid content of individual trichomes or by the shift in the ratio between mono- and sesquiterpenes. Blocking the complete MEP pathway at a downstream step (4-(cytidine-5′-diphospho)-2-*C*-methyl-D-erythritol kinase, CMK) in *Nicotiana benthamiana* also resulted in increased trichome densities among other phenotypes (Ahn and Pai, 2008). The increase in trichomes in plants with reduced expression of either *CMK* or *SlDXS2* might thus be a compensation mechanism for reduced isoprenoid flux to isoprenoid defense compounds. Hence, metabolic alterations may be another trigger for a highly flexible adaptation in the development of trichomes with respect to their densities, distribution of various types, morphology, and other features. Comparable links between the chemical content of tomato trichomes (insecticidal methylketones, sesquiterpenes) and their morphological characteristics or densities have recently been reported (Ben-Israel et al., 2009; Kang et al., 2010). However, we cannot exclude that the increased ratio of sesquiterpenes to monoterpenes or another unknown factor altered by the RNAi approach has caused the change in feeding behavior and the alteration in glandular trichome numbers.

In summary, the alterations in isoprenoid biosynthesis and developmental responses observed in trichomes of transgenic tomato plants upon interfering with *SlDXS2* gene expression illustrate the enormous plasticity of plants to adapt to metabolic changes and to make the best use of available isoprenoid precursors. The feedback responses appear to be threefold: (1) adaptation of isoprenoid profiles to produce less MEP-dependent compounds, (2) replacement to some extent of MEP-derived precursors by MVA-derived precursors for isoprenoid biosynthesis, and (3) up-regulation of trichome numbers when production in individual trichomes is compromised. The finding that up-regulation of *SlDXS1* does not seem to constitute an alternative strategy underscores the important, non-redundant role of DXS2 in plant isoprenoid metabolism.

METHODS

Plant Cultivation, Trichome Procedures, and Caterpillar Feeding Conditions

Tomato (*Solanum lycopersicum*) cv. Moneymaker plants (seed origin N.L. Chrestensen, Erfurt, Germany) were grown on soil at 24°C day/21°C night regimes on a 16-h daily light period at 65% humidity in a greenhouse.

Trichome isolation followed the method of Gershenzon et al. (1992). In brief, 60 g of young leaf material was immersed in cold 5 mM aurintricarboxylic acid/1 mM thiourea for 1 h. The material was treated in a beadbeater with 140 g glass beads (diameter 0.5 mm), 35 g Amberlite XAD-4 and buffer (25 mM HEPES pH 7.3, 200 mM sorbitol, 10 mM sucrose, 5 mM ATA, 1 mM thiourea, 0.6% methyl cellulose, 1% polyvinylpyrrolidone). Beating was performed three times at a 90-V setting for 1 min with 1 min of cooling in between. Homogenized material was filtered through a 350-μm mesh filter, flow-through was removed from debris by filtration through a mesh with 105-μm pore size and trichomes were collected on a 40-μm mesh filter. The procedure was carried out in a cold lab.

The number of glandular trichomes was determined from the adaxial surface of 2-cm-long leaflets of the same developmental stage under a stereomicroscope. The area evaluated was standardized to 90 mm^2 in the leaf center at the midrib. Environmental Scanning Electron Microscopy (ESEM) analysis was carried out in a wet atmosphere on a Philips ESEM XL30 FEG. Pollen germination was carried out according to Li et al. (2004).

For concomitant headspace analysis of volatiles and evaluation of herbivore attractiveness of leaves, 5-week-old tomato plants (including pot) were placed in Nalophan® plastic bags (Kalle GmbH, Wiesbaden) and infested with four to six *Spodoptera littoralis* larvae (third instar) per plant. Herbivore damage was calculated as cm^2 of leaf area consumed.

SlDXS Isogene Cloning and Expression in *Escherichia coli*

Specific primer pairs for PCR amplification of coding sequences were derived from available sequences (AF143812, *SlDXS1 S. lycopersicum*; AY687353, *ShDXS2 S. habrochaites*): *SlDXS1*-fw-5′-AGTGACAGTAGCACCAACACAC-3′; *SlDXS1*-re-5′-CAAAGACT AACACCATTGGCCAAGA-3′ and *SlDXS2*-fw-5′-ATGGCAGTTTC TTCAGGCACTGTATTTAG-3′; *SlDXS2*-re-5′-TTCACCAACACTTTC TGCAATATGATC-3′. Amplicons were obtained from cDNA and genomic DNA as templates using Platinum® PCR SuperMix High Fidelity polymerase (Invitrogen, Carlsbad, USA) and cloned into pGEM-T Easy vector (Promega, Madison, USA). The 5′ upstream regions were isolated from genomic DNA using a GenomeWalker Kit (Clontech, Mountain View, USA) according to the manufacturer's instructions.

To determine the functionality of the cloned *DXS* sequences, regions covering the mature protein without the transit peptide were amplified using *SlDXS1*ex-fw-5′-GAAAATGGCTTTGTGTGCT-TATGCATTTCCTGG-3′, *SlDXS1*ex-re-5′-TTATGTCATAACCTCTA-GAGCCTCTCTGGTTTG-3′ and *SlDXS2*-ex-fw-5′-AGTTTGCAGATT GATTTTTCAG-3′, *SlDXS2*-ex-re-5′-TTAGTTTACTACCATAGCTT CTTTTG-3′. Amplicons were cloned into the pQE60 expression vector (Qiagen, Hilden, Germany). Plasmids were used to complement the *dxs*-deficient *E. coli* strain EcAB4-2 to overcome its requirement of mevalonate for isoprenoid synthesis and survival (Sauret-Güeto et al., 2006).

The above-mentioned primer pairs were used to clone both *SlDXS* sequence into the His-tag containing over-expression vector pET28a(+) (Novagen). After transformation into *E. coli* BL21(DE3)RIL (Stratagene), induction of culture in LB media was carried out with 1 mM IPTG at the OD of 0.6 followed by overnight cultivation at 4°C. Centrifugation (4°C, 15 min, 5000 *g*) separated the bacterial cells from the media. Washing of cells was performed with 30 mM NaH_2PO_4 (pH 7.5) 100 mM NaCl, 2.5 mM 2-mercapto-ethanol prior to sonification (three times, 30 s, 60% power with UW 2070 (Bandelin)). The soluble fraction was used for affinity purification with TALON-Matrix (BD Bioscience). Elution was carried out with high-imidazole-buffer (30 mM NaH_2PO_4 (pH 7.5) 100 mM NaCl, 2.5 mM 2-mercapto-ethanol, 250 mM imidazole, 1 mM thiamine-diphosphate, 2.5 mM $MgCl_2$) after washing with two low-imidazole buffers (buffer 1: 30 mM NaH_2PO_4 (pH 7.5) 100 mM NaCl, 2.5 mM 2-mercapto-ethanol, 40 mM imidazole, 1 mM thiamine-diphosphate, 2.5 mM $MgCl_2$; buffer 2: 30 mM NaH_2PO_4 (pH 7.5) 100 mM NaCl, 2.5 mM 2-mercapto-ethanol, 40 mM imidazole, 1 mM thiamine-diphosphate, 2.5 mM $MgCl_2$).

RNA, DNA, and Protein Isolation and Analytical Procedures

RNA and genomic DNA were isolated from frozen ground plant material, using RNeasy Plant Minikit, DNeasy kit, and enzymes from Qiagen. For RNA isolation, material was homogenized in RLT-buffer and treated with DNase I. Reverse transcription reaction was carried out with 1 μg of total RNA using the Omniscript RT Kit (Qiagen) according to the supplier's instructions.

Real-time RT–PCR was carried out using a SYBR Green assay (Applied Biosystems, Foster City, USA) on an Mx3000P or 3005P QPCR system (Stratagene, La Jolla, USA) as previously described (Floss et al., 2008). Each 10-μl assay contained 100 nM of primer, 5 μl SYBR Green mix, and 5 ng RNA. Real-time primer pairs were derived from the two *SlDXS* genes (*SlDXS1*-fw-5′-AACCTTTGCTGCTGGATTGG-3′ and re5′-TCAACGTCATGCACTACCTGG-3′; *SlDXS2*-fw5′-AGCAGGCT-TAGCTACAGAAGG-3′ and re5′–CGTCTGCACCTACCAAACC-3′) and also from *SlAOC*-fw5′–TTCTACTTCGGCGATTACGGTC-3′ and *SlAOC*-re5′-GGTTAAGTACGCTCCCTGAACG-3′. The relative mRNA abundance was calculated by using the comparative C_T method (Pfaffl, 2001) and normalization to elongation factor 1 alpha (X14449) amplified using *SlEF*-fw5′–GCTGCTGTAACAA-GATGGATGC-3′ and re5′-AGGGTTGTAACCAACCTTCTTGAA-3′.

The antibodies to SlDXS2-specific peptides were raised by Eurogentec (Seraing, Belgium). Two peptides from the N- and the C-terminus (SLQIDFSGEK and LTLLGRPKEAMVVN) were used to immunize rabbits. Antibodies were purified

against the respective peptides. For the determination of SlDXS2 protein abundance in plant extracts, total protein was isolated from tomato plant organs according to Meyer et al. (1988). Proteins were dissolved in sample buffer (70 mM Tris-buffer pH 8.0, 1% glycerol, 2% SDS, 0.05% 2-mercaptoethanol) and boiled for 3 min. Five μg protein were separated on 10% acrylamide gels and blotted onto nitrocellulose. After blocking by 5% BSA in TBST buffer, the anti-DXS2 antibody was applied in a 1:1000 dilution followed by three washing steps. Goat anti-rabbit IgG coupled to alkaline phosphatase (Chemicon) were used as secondary antibody. Detection was performed by Nitroblue Tetrazolium (NBT)/ 5-bromo-4-chloro-3-indolyl phosphate, p-toluidine salt (BCIP) staining.

For immunodetection of SlDXS2 on plant leaves, this material was fixed and embedded in PEG (polyethylene glycol) as described by Hause et al. (1996). Sections of 3-μm thickness were immunolabeled with SlDXS2 antibody diluted 1:250 in 5% BSA containing 1% acetylated BSA (Aurion, Wageningen, Netherlands). As control, the antibody was saturated 1000 times with peptides prior to immunolabeling. The goat anti-rabbit IgG antibody was used in a dilution of 1:250. Detection was carried out with NBT/BCIP staining.

Generation of *SlDXS2* RNAi Plants

A fragment of 262 bp was amplified from the 3′-UTR including few nucleotides from the C-terminal coding region with primer pair *SlDXS2*RNAi-fw-5′–AACTAAATTTCCAAAAGGCTATAAG-3′ and *SlDXS2*RNAi-re-5′-GTAGATTTAACAGTATGATTACTACG-3′ containing *attB* recombination site for Gateway® cloning. The fragment was amplified using Platinum® PCR SuperMix High Fidelity, cloned into pDONR (Invitrogen), and further transferred into the RNAi vector pHellsgate 8 (Wesley et al., 2001). For transformation control, the *ccdB* genes of pHellsgate were cut out by *Xba*I and *Xho*I. After filling in, re-ligation was performed to receive the control plasmid without the RNAi cassette. After transformation of both plasmids into *Agrobacterium tumefaciens*, GV3101 cotyledons of etiolated 14-day-old tomato plants were incubated in bacterial suspension. Subsequent procedures generating calli, shoots, and roots were carried out according to Ling et al. (1998). T_0 transformants were propagated by cuttings.

Metabolite Collection and Analyses

To collect trichome isoprenoids, 5-mm-long PDMS tubes (1.5 mm i.d. × 2.3 mm o.d., Reichelt Chemietechnik, Heidelberg, Germany) were mounted on 5-cm-long glass rods (1.5 mm o.d.) and conditioned for 15 min at 250°C in a Helium stream. The preconditioned collecting device was gently moved three times over the adaxial surface of the leaf. Chosen leaves had the same age and size. All collections were performed within 10 min. After the collection, each collecting device was stored in an individual glass vial and was then transferred to a capped glass liner fitting to the thermal desorption injector (see below). An automatic liner change for thermal desorption was achieved with a CONCEPT autosampler (PAS Technologies, Magdala, Germany).

Determination of the isotopic ratios and concentrations of the volatiles was achieved on a GC–C–IRMS system consisting of an HP 6890 (Agilent Technologies, Santa Clara, USA) equipped with an Optic 3 injector (ATAS Benelux B.V., Zoetermeer, Netherlands) as thermal desorption inlet, a combustion furnace, and an isotope ratio mass spectrometer (IsoPrime, Micromass, Manchester, UK). Volatiles were separated on a ZB-5ms fused silica column (30 m × 0.25 mm i.d. × 0.25-μm film, Phenomenex, Torrance, USA) using helium as carrier gas with a linear flow rate of 1 ml min^{-1}. The column oven was maintained at 45°C for 2 min, with an increase of 10°C min^{-1} to 260°C, then with an increase of 30°C min^{-1} to 280°C, maintained for 2 min. The eluting compounds were combusted online at 850°C on copper oxide and the resulting CO_2 was transferred into the mass spectrometer after removing the water by a Nafion® tube gas drying system. For identification of the eluting volatiles, a 10% aliquot of the sample was split before combustion but after separation and transferred into a time-of-flight mass spectrometer (GCT, Micromass, Manchester, UK). Relative concentrations were calculated based on the area of the *m/z* 44 signal of the IRMS and normalized to the individual number of C-atoms in the molecules (β-phellandrene $C_{10}H_{16}$, (*E*)-β-caryophyllene, and α-humulene $C_{15}H_{24}$) reflecting the relatively produced amount of CO_2. Quantitative determinations of isoprenoids were carried out based on the produced CO_2 using a one-point calibration with decane as an external standard and calculated for collected pmoles of compounds. Calculations of total peak areas or total ng of compounds gave very similar results.

For IRMS, the system was calibrated and checked with a mixture of reference compounds with known $\delta^{13}C$ values (SE $\leqslant 0.2‰$) calibrated on the international VPDB (Vienna Pee Dee Belemnite) scale using IAEA reference material, NBS 22, with a $\delta^{13}C$ value of –30.03‰ (Coplen et al., 2006; Werner and Brand, 2001). All isotope ratios are given as $\delta^{13}C$ values defined as follows: $\delta^{13}C = (R_{sample}/ R_{standard}) - 1$, where R corresponds to the ^{13}C to ^{12}C ratio of the sample and the standard, respectively. Isotopic ratios are expressed in δ notation versus the international (hypothetical) VPDB standard and given in ‰ according to the relation:

$$\delta^{13}C_{VPDB} = \frac{\left(^{13}C/^{12}C\right)_{sample} - \left(^{13}C/^{12}C\right)_{VPDB}}{\left(^{13}C/^{12}C\right)_{VPDB}} \times 1000(‰),$$

where $\Delta\delta^{13}C$ represents the difference between $\delta^{13}C$ values.

During evaluation of herbivore feeding, the emitted volatiles were trapped by continuously circulating air through a charcoal filter (1.5 mg charcoal, CLSA-Filter, Gränicher and Quartero, Daumazan sur Arize, France) for 48 h. The collected volatiles were eluted with dichloromethane (2 × 20 μl) containing n-bromodecane (100 μg ml^{-1}) as internal standard. GC–MS analysis was performed on a TRACE GC 2000 with a TRACE MS (ThermoQuest/Finnigan Bremen, Germany)

equipped with a ZB-5 capillary column (15 m × 0.25 mm i.d. with 0.25-μm film, Phenomenex, Torrance, USA). One μl of the sample was injected in splitless mode at an injection port temperature of 220°C. The oven temperature was kept at 45°C for 2 min followed by a ramp of 10°C min^{-1} to 200°C followed by an additional ramp of 30°C min^{-1} to 280°C and a final time of 1 min. Helium at a flow rate of 1.5 ml min^{-1} served as carrier gas. Ionization potential was set to 70 eV, and scanning was performed from 40 to 450 amu. The headspace volatiles were identified by comparing their mass spectra and Kovats indices with authentic standards.

Statistical Analysis

The significance of all experiments was determined with One-Way ANOVA combined with post hoc Tukey-HSD test. All bars in one diagram marked with the same letter belong to the same group of significance. All statistical analyses were performed using VassarStat (http://faculty.vassar.edu/lowry/VassarStats.html) or SPSS 13.0 (SPSS Inc., Chicago, IL, USA).

Accession Numbers

Sequence data from this article can be found in the EMBL/GenBank data libraries under accession numbers FN424051 and FN424052.

SUPPLEMENTARY DATA

Supplementary Data are available at Molecular Plant Online.

FUNDING

This work was supported in part by the Deutsche Forschungsgemeinschaft (Bonn, Germany) by grant WA 536/5–1.

ACKNOWLEDGMENTS

We thank F. Syrowatka (Interdisciplinary Center of Materials Science, Halle) for performing ESEM analyses and P. Waterhouse (University of Sydney) for providing pHellsgate8. The skillful technical assistance of K. Manke is gratefully acknowledged. No conflict of interest declared.

REFERENCES

Ahn, C.S., and Pai, H.S. (2008). Physiological function of *IspE*, a plastid MEP pathway gene for isoprenoid biosynthesis, in organelle biogenesis and cell morphogenesis in *Nicotiana benthamiana*. Plant Mol. Biol. **66,** 503–517.

Arigoni, D., Sagner, S., Latzel, C., Eisenreich, W., Bacher, A., and Zenk, M.H. (1997). Terpenoid biosynthesis from 1-deoxy-D-xylulose in higher plants by intramolecular skeletal rearrangement. Proc. Natl Acad. Sci. U S A. **94,** 10600–10605.

Arimura, G.I., Garms, S., Maffei, M., Bossi, S., Schulze, B., Leitner, M., Mithoefer, A., and Boland, W. (2008). Herbivore-induced terpenoid emission in *Medicago truncatula*: concerted action of jasmonate, ethylene and calcium signaling. Planta. **227,** 453–464.

Bartram, S., Jux, A., Gleixner, G., and Boland, W. (2006). Dynamic pathway allocation in early terpenoid biosynthesis of stress-induced lima bean leaves. Phytochemistry. **67,** 1661–1672.

Battilana, J., Costantini, L., Emanuelli, F., Sevini, F., Segala, C., Moser, S., Velasco, R., Versini, G., and Grando, M.S. (2009). The *1-deoxy-D-xylulose 5-phosphate synthase* gene co-localizes with a major QTL affecting monoterpene content in grapevine. Theor. Appl. Genet. **118,** 653–669.

Ben-Israel, I., Yu, G., Austin, M.B., Bhuiyan, N., Auldridge, M., Nguyen, T., Schauvinhold, I., Noel, J.P., Pichersky, E., and Fridman, E. (2009). Multiple biochemical and morphological factors underlie the production of methylketones in tomato trichomes. Plant Physiol. **151,** 1952–1964.

Besser, K., Harper, A., Welsby, N., Schauvinhold, I., Slocombe, S., Li, Y., Dixon, R.A., and Broun, P. (2009). Divergent regulation of terpenoid metabolism in the trichomes of wild and cultivated tomato species. Plant Physiol. **149,** 499–514.

Boughton, A.J., Hoover, K., and Felton, G.W. (2005). Methyl jasmonate application induces increased densities of glandular trichomes on tomato, *Lycopersicon esculentum*. J. Chem. Ecol. **31,** 2211–2216.

Carretero-Paulet, L., Cairo, A., Botella-Pavia, P., Besumbes, O., Campos, N., Boronat, A., and Rodríguez-Concepción, M. (2006). Enhanced flux through the methylerythritol 4-phosphate pathway in *Arabidopsis* plants overexpressing deoxyxylulose 5-phosphate reductoisomerase. Plant Mol. Biol. **62,** 683–695.

Chappell, J. (2002). The genetics and molecular genetics of terpene and sterol origami. Curr. Opin. Plant Biol. **5,** 151–157.

Coplen, T.B., Brand, W.A., Gehre, M., Groning, M., Meijer, H.A.J., Toman, B., and Verkouteren, R.M. (2006). New guidelines for delta C-13 measurements. Anal. Chem. **78,** 2439–2441.

Cordoba, E., Salmi, M., and León, P. (2009). Unravelling the regulatory mechanisms that modulate the MEP pathway in higher plants. J. Exp. Bot. **60,** 2933–2943.

Duchêne, E., Butterlin, G., Claudel, P., Dumas, V., Jaegli, N., and Merdinoglu, D. (2009). A grapevine (*Vitis vinifera* L.) *deoxy-D-xylulose synthase* gene colocates with a major quantitative trait loci for terpenol content. Theor. Appl. Genet. **118,** 541–552.

Dudareva, N., Andersson, S., Orlova, I., Gatto, N., Reichelt, M., Rhodes, D., Boland, W., and Gershenzon, J. (2005). The nonmevalonate pathway supports both monoterpene and sesquiterpene formation in snapdragon flowers. Proc. Natl Acad. Sci. U S A. **102,** 933–938.

Enfissi, E.M.A., Fraser, P.D., Lois, L.M., Boronat, A., Schuch, W., and Bramley, P.M. (2005). Metabolic engineering of the mevalonate and non-mevalonate isopentenyl diphosphate-forming pathways for the production of health-promoting isoprenoids in tomato. Plant Biotechnol. J. **3,** 17–27.

Estévez, J.M., Cantero, A., Reindl, A., Reichler, S., and León, P. (2001). 1-deoxy-D-xylulose-5-phosphate synthase, a limiting enzyme for plastidic isoprenoid biosynthesis in plants. J. Biol. Chem. **276,** 22901–22909.

Estévez, J.M., Cantero, A., Romero, C., Kawaide, H., Jimenez, L.F., Kuzuyama, T., Seto, H., Kamiya, Y., and León, P. (2000). Analysis of the expression of *CLA1*, a gene that encodes the 1-deoxyxylulose 5-phosphate synthase of the 2-C-methyl-D-erythritol-4-phosphate pathway in *Arabidopsis*. Plant Physiol. **124,** 95–103.

Floss, D.S., Hause, B., Lange, P.R., Küster, H., Strack, D., and Walter, M.H. (2008). Knock-down of the MEP pathway isogene *1-deoxy-D-xylulose 5-phosphate synthase 2* inhibits formation of arbuscular mycorrhiza-induced apocarotenoids, and abolishes normal expression of mycorrhiza-specific plant marker genes. Plant J. **56,** 86–100.

Galpaz, N., Ronen, G., Khalfa, Z., Zamir, D., and Hirschberg, J. (2006). A chromoplast-specific carotenoid biosynthesis pathway is revealed by cloning of the tomato *white-flower* locus. Plant Cell. **18,** 1947–1960.

Gershenzon, J., McCaskill, D., Rajaonarivony, J.I.M., Mihaliak, C., Karp, F., and Croteau, R. (1992). Isolation of secretory-cells from plant glandular trichomes and their use in biosynthetic studies of monoterpenes and other gland products. Anal. Biochem. **200,** 130–138.

Grassi, P., Novak, J., Steinlesberger, H., and Franz, C. (2004). A direct liquid, non-equilibrium solid-phase micro-extraction application for analysing chemical variation of single peltate trichomes on leaves of *Salvia officinalis*. Phytochem. Anal. **15,** 198–203.

Hause, B., Demus, U., Teichmann, C., Parthier, B., and Wasternack, C. (1996). Developmental and tissue-specific expression of JIP-23, a jasmonate-inducible protein of barley. Plant Cell Physiol. **37,** 641–649.

Hemmerlin, A., Hoeffler, J.F., Meyer, O., Tritsch, D., Kagan, I.A., Grosdemange-Billiard, C., Rohmer, M., and Bach, T.J. (2003). Cross-talk between the cytosolic mevalonate and the plastidial methylerythritol phosphate pathways in Tobacco Bright Yellow-2 cells. J. Biol. Chem. **278,** 26666–26676.

Jux, A., Gleixner, G., and Boland, W. (2001). Classification of terpenoids according to the methylerythritolphosphate or the mevalonate pathway with natural C-12/C-13 isotope ratios: Dynamic allocation of resources in induced plants. Angew. Chem.-Int. Edit. **40,** 2091–2093.

Kang, J.H., Shi, F., Jones, A.D., Marks, M.D., and Howe, G.A. (2010). Distortion of trichome morphology by the hairless mutation of tomato affects leaf surface chemistry. J. Exp. Bot. **61,** 1053–1064.

Khemvong, S., and Suvachittanont, W. (2005). Molecular cloning and expression of a cDNA encoding 1-deoxy-D-xylulose-5-phosphate synthase from oil palm *Elaeis guineensis* Jacq. Plant Sci. **169,** 571–578.

Kim, S.M., Kuzuyama, T., Chang, Y.J., Song, K.S., and Kim, S.U. (2006). Identification of class 2 *1-deoxy-D-xylulose 5-phosphate synthase* and *1-deoxy-D-xylulose 5-phosphate reductoisomerase* genes from *Ginkgo biloba* and their transcription in embryo culture with respect to ginkgolide biosynthesis. Planta Med. **72,** 234–240.

Kim, Y.B., Kim, S.M., Kang, M.K., Kuzuyama, T., Lee, J.K., Park, S.C., Shin, S.C., and Kim, S.U. (2009). Regulation of resin acid synthesis in *Pinus densiflora* by differential transcription of genes encoding multiple 1-deoxy-D-xylulose 5-phosphate synthase and 1-hydroxy-2-methyl-2-(E)-butenyl 4-diphosphate reductase genes. Tree Physiol. **29,** 737–749.

Kishimoto, S., and Ohmiya, A. (2006). Regulation of carotenoid biosynthesis in petals and leaves of chrysanthemum (*Chrysanthemum morifolium*). Physiol. Plant. **128,** 436–447.

Lange, B.M., Rujan, T., Martin, W., and Croteau, R. (2000). Isoprenoid biosynthesis: The evolution of two ancient and distinct pathways across genomes. Proc. Natl Acad. Sci. U S A. **97,** 13172–13177.

Lange, B.M., Wildung, M.R., McCaskill, D., and Croteau, R. (1998). A family of transketolases that directs isoprenoid biosynthesis via a mevalonate-independent pathway. Proc. Natl Acad. Sci. U S A. **95,** 2100–2104.

Laule, O., Fürholz, A., Chang, H.S., Zhu, T., Wang, X., Heifetz, P.B., Gruissem, W., and Lange, B.M. (2003). Crosstalk between cytosolic and plastidial pathways of isoprenoid biosynthesis in *Arabidopsis thaliana*. Proc. Natl Acad. Sci. U S A. **100,** 6866–6871.

Li, L., Zhao, Y.F., McCaig, B.C., Wingerd, B.A., Wang, J.H., Whalon, M.E., Pichersky, E., and Howe, G.A. (2004). The tomato homolog of *CORONATINE-INSENSITIVE1* is required for the maternal control of seed maturation, jasmonate-signaled defense responses, and glandular trichome development. Plant Cell. **16,** 126–143.

Ling, H.Q., Kriseleit, D., and Ganal, M.W. (1998). Effect of ticarcillin potassium clavulanate on callus growth and shoot regeneration in Agrobacterium-mediated transformation of tomato (*Lycopersicon esculentum* Mill.). Plant Cell Rep. **17,** 843–847.

Lois, L.M., Rodríguez-Concepción, M., Gallego, F., Campos, N., and Boronat, A. (2000). Carotenoid biosynthesis during tomato fruit development: regulatory role of 1-deoxy-D-xylulose 5-phosphate synthase. Plant J. **22,** 503–513.

Maluf, W.M., Inoue, I.F., Ferreira, R. de P.D., Gomes, L.A.A., de Castro, E.M., and Cardoso, M. das G. (2007). Higher glandular trichome density in tomato leaflets and repellence to spider mites. Pesqu. Agropec. Brasil. **42,** 1227–1235.

Mandel, M.A., Feldmann, K.A., Herrera-Estrella, L., RochaSosa, M., and León, P. (1996). *CLA1*, a novel gene required for chloroplast development, is highly conserved in evolution. Plant J. **9,** 649–658.

Meyer, Y., Grosset, J., Chartier, Y., and Cleyetmarel, J.C. (1988). Preparation by two-dimensional electrophoresis of proteins for antibody-production: antibodies against proteins whose synthesis is reduced by auxin in tobacco mesophyll protoplasts. Electrophoresis. **9,** 704–712.

Moehs, C.P., Tian, L., Osteryoung, K.W., and DellaPenna, D. (2001). Analysis of carotenoid biosynthetic gene expression during marigold petal development. Plant Mol. Biol. **45,** 281–293.

Morris, W.L., Ducreux, L.J.M., Hedden, P., Millam, S., and Taylor, M.A. (2006). Overexpression of a bacterial *1-deoxy-D-xylulose 5-phosphate synthase* gene in potato tubers perturbs the isoprenoid metabolic network: implications for the control of the tuber life cycle. J. Exp. Bot. **57,** 3007–3018.

Muñoz-Bertomeu, J., Arrillaga, I., Ros, R., and Segura, J. (2006). Up-regulation of *1-deoxy-D-xylulose-5-phosphate synthase* enhances production of essential oils in transgenic spike lavender. Plant Physiol. **142,** 890–900.

Nagata, N., Suzuki, M., Yoshida, S., and Muranaka, T. (2002). Mevalonic acid partially restores chloroplast and etioplast development in *Arabidopsis* lacking the non-mevalonate pathway. Planta. **216,** 345–350.

Narita, J.O., and Gruissem, W. (1989). Tomato hydroxymethylglutaryl-CoA reductase is required early in fruit-development but not during ripening. Plant Cell. **1,** 181–190.

Nieto, B., Fores, O., Arro, M., and Ferrer, A. (2009). *Arabidopsis* 3-hydroxy-3-methylglutaryl-CoA reductase is regulated at the post-translational level in response to alterations of the sphingolipid and the sterol biosynthetic pathways. Phytochemistry. **70,** 53–59.

Okada, A., Shimizu, T., Okada, K., Kuzuyama, T., Koga, J., Shibuya, N., Nojiri, H., and Yamane, H. (2007). Elicitor induced activation of the methylerythritol phosphate pathway toward phytoalexins biosynthesis in rice. Plant Mol. Biol. **65,** 177–187.

Pfaffl, M.W. (2001). A new mathematical model for relative quantification in real-time RT–PCR. Nucleic Acids Res. **29.**

Phillips, M.A., et al. (2007). Functional identification and differential expression of *1-deoxy-D-xylulose 5-phosphate synthase* in induced terpenoid resin formation of Norway spruce (*Picea abies*). Plant Mol. Biol. **65,** 243–257.

Phillips, M.A., León, P., Boronat, A., and Rodríguez-Concepción, M. (2008). The plastidial MEP pathway: unified nomenclature and resources. Trends Plant Sci. **13,** 619–623.

Rodríguez-Concepción, M. (2006). Early steps in isoprenoid biosynthesis: multilevel regulation of the supply of common precursors in plant cells. Phytochem. Rev. **5,** 1–15.

Rodríguez-Concepción, M., and Boronat, A. (2002). Elucidation of the methylerythritol phosphate pathway for isoprenoid biosynthesis in bacteria and plastids: a metabolic milestone achieved through genomics. Plant Physiol. **130,** 1079–1089.

Sallaud, C., et al. (2009). A novel pathway for sesquiterpene biosynthesis from Z, Z-farnesyl pyrophosphate in the wild tomato *Solanum habrochaites*. Plant Cell. **21,** 301–317.

Sánchez-Hernández, C., López, M.G., and Délano-Frier, J.P. (2006). Reduced levels of volatile emissions in jasmonate-deficient *spr2* tomato mutants favour oviposition by insect herbivores. Plant Cell Environ. **29,** 546–557.

Sando, T., Takeno, S., Watanabe, N., Okumoto, H., Kuzuyama, T., Yamashita, A., Hattori, M., Ogasawara, N., Fukusaki, E., and Kobayashi, A. (2008). Cloning and characterization of the 2-C-methyl-D-erythritol 4-phosphate (MEP) pathway genes of a natural-rubber producing plant, *Hevea brasiliensis*. Biosci. Biotechnol. Biochem. **72,** 2903–2917.

Sauret-Güeto, S., Urós, E.M., Ibánez, E., Boronat, A., and Rodríguez-Concepción, M. (2006). A mutant pyruvate dehydrogenase El subunit allows survival of *Escherichia coli* strains defective in 1-deoxy-D-xylulose 5-phosphate synthase. FEBS Lett. **580,** 736–740.

Schilmiller, A.L., Schauvinhold, I., Larson, M., Xu, R., Charbonneau, A.L., Schmidt, A., Wilkerson, C., Last, R.L., and Pichersky, E. (2009). Monoterpenes in the glandular trichomes of tomato are synthesized from a neryl diphosphate precursor rather than geranyl diphosphate. Proc. Natl Acad. Sci. U S A. **106,** 10865–10870.

Schmiderer, C., Grassi, P., Novak, J., Weber, M., and Franz, C. (2008). Diversity of essential oil glands of clary sage (*Salvia sclarea* L., Lamiaceae). Plant Biol. **10,** 433–440.

Schuhr, C.A., Radykewicz, T., Sagner, S., Latzel, C., Zenk, M.H., Arigoni, D., Bacher, A., Rohdich, F., and Eisenreich, W. (2003). Quantitative assessment of crosstalk between the two isoprenoid biosynthesis pathways in plants by NMR spectroscopy. Phytochem. Rev. **2,** 3–16.

Simmons, A.T., and Gurr, G.M. (2005). Trichomes of *Lycopersicon* species and their hybrids: effects on pests and natural enemies. Agric. For. Entomol. **7,** 265–276.

Stermer, B.A., Bianchini, G.M., and Korth, K.L. (1994). Regulation of Hmg-CoA reductase-activity in plants. J. Lipid Res. **35,** 1133–1140.

Totte, N., Van den Ende, W., Van Damme, E.J.M., Compernolle, F., Baboeuf, I., and Geuns, J.M.C. (2003). Cloning and heterologous expression of early genes in gibberellin and steviol biosynthesis via the methylerythritol phosphate pathway in *Stevia rebaudiana*. Can. J. Bot.–Rev. Can. Bot. **81,** 517–522.

Towler, M.J., and Weathers, P.J. (2007). Evidence of artemisinin production from IPP stemming from both the mevalonate and the nonmevalonate pathways. Plant Cell Rep. **26,** 2129–2136.

Tretner, C., Huth, U., and Hause, B. (2008). Mechanostimulation of *Medicago truncatula* leads to enhanced levels of jasmonic acid. J. Exp. Bot. **59,** 2847–2856.

Vallabhaneni, R., and Wurtzel, E.T. (2009). Timing and biosynthetic potential for carotenoid accumulation in genetically diverse germplasm of maize. Plant Physiol. **150,** 562–572.

Walter, M.H., Hans, J., and Strack, D. (2002). Two distantly related genes encoding 1-deoxy-D-xylulose 5-phosphate synthases: differential regulation in shoots and apocarotenoid-accumulating mycorrhizal roots. Plant J. **31,** 243–254.

Werner, R.A., and Brand, W.A. (2001). Referencing strategies and techniques in stable isotope ratio analysis. Rapid Commun. Mass Spectrom. **15,** 501–519.

Wesley, S.V., et al. (2001). Construct design for efficient, effective and high-throughput gene silencing in plants. Plant J. **27,** 581–590.

Ziegler, J., Stenzel, I., Hause, B., Maucher, H., Hamberg, M., Grimm, R., Ganal, M., and Wasternack, C. (2000). Molecular cloning of allene oxide cyclase: the enzyme establishing the stereochemistry of octadecanoids and jasmonates. J. Biol. Chem. **275,** 19132–19138.